3D-Printed Strain Gauges Based on Conductive Filament for Experimental Stress Analysis

Romol Chadda[1], Omar Ben Dali[1], Bastian Latsch[1], Esan Sundaralingam[1], and Mario Kupnik[1]
[1]Measurement and Sensor Technology Group, Technical University of Darmstadt, Germany
romol.chadda@tu-darmstadt.de

***Abstract*—We present a method for manufacturing 3D-printed strain gauges by means of fused filament fabrication that are suitable for experimental stress analysis applications. The 3D-printed strain gauge (SG) is based on a multilayer structure, which is similar to the design of conventional metal foil SGs. This involves printing a meander-shaped measuring grid layer consisting of a conductive compound filament on a layer of non-conductive PLA that serves as a substrate. In order to evaluate the strain sensing behavior of the 3D-printed SG, it is bonded onto a steel plate by means of a cold curing superglue that undergoes a bending load of 30 N. Here, a finite element analysis is conducted for determining a proper position that ensures a high strain while not exceeding the yield strength. Our results show a reproducible behavior of the change in resistance of the 3D-printed SG in response to the bending load. Despite an existing creep that is based on the polymer properties of the filament, a linear behavior of the change in resistance linearity error of ±4 % is present. Furthermore, the sensitivity of the 3D-printed SG is four times higher than that of conventional metal foil strain gauges. Thus, these results confirm that the 3D-printed SG is a cost-effective alternative for strain sensing applications.**

***Index Terms*—strain gauge, force sensing, 3D-printed**

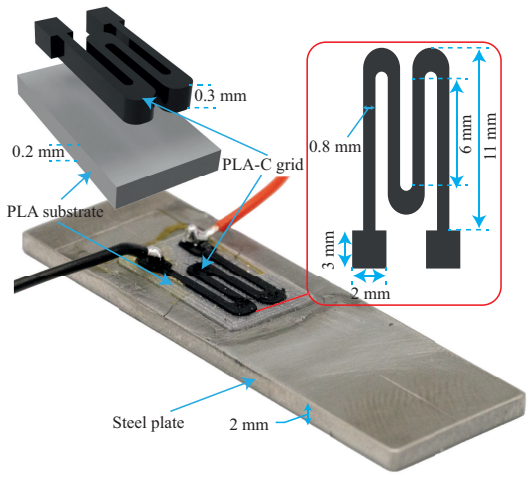

Fig. 1. The 3D-printed SG is based on a PLA substrate and a measuring grid made of conductive PLA. It is applied with a cold-curing superglue to a steel plate, which serves as spring element.

I. Introduction

Strain gauges (SGs) are one of the most fundamental sensing devices [1] and enable the conversion of a strain into an electrical signal [2]. Typically, the conversion results from a change in resistance into an electrical voltage by means of a Wheatstone bridge [1]. They are used in transducer applications for measuring strain, force, pressure or torque [3] as well as for experimental stress analysis for structural health monitoring [4], [5]. The most established technologies for realizing SGs include metal foil SGs, thin-film SGs, thick-film SGs and semiconductor SGs [6]. In addition to these well-established technologies, the realization of printed SGs have recently been investigated, providing an additional but cost effective alternative method for strain measurement. In the state of the art, several approaches have been introduced, where mostly aerosol or inkjet printing techniques are used to apply a meander-shaped structure to a 3D-printed spring element [7]–[11]. More recently, approaches based on 3D-printed SGs made of conductive filament that are directly printed on a 3D-printed spring element by means of fused filament fabrication (FFF) have been proven to be a promising route for sensor-integration [12], [13], while being cost-effective. However, 3D-printed SGs manufactured by FFF have not been bonded to metallic spring elements as in the conventional method by using metal foil SGs and investigated regarding their strain response. Therefore, an approach for manufacturing 3D-printed SGs made of conductive filament is presented in this work, which can be bonded to a structure that is loaded. This provides a strain measurement, which is a typical use case in experimental stress analysis applications for conventional SG.

The work has been funded by the Deutsche Forschungsgemeinschaft (DFG) under grant numbers 418628981 and 450821862 within the research training group 2761.

II. Design and Fabrication of the 3D-Printed Strain Gauge

In order to use the 3D-printed strain gauge (SG) as a conventional SG, a two-layer design based on a substrate layer and a measuring grid layer is used (Fig. 1). The meander-shaped measuring grid consists of four tracks and an effective length of 6 mm. For minimizing the impact of cross-sensitivity, the end loops are designed to feature a larger width than the measuring grid line width [1], [14]. The outer and inner radii of the end loops are 1 mm and 0.4 mm, respectively, corresponding to a U-shape as in the case of conventional SGs. This design is prepared for FFF using the open source software PrusaSlicer (Prusa Research a.s., Prague, Czech Republic). Here, a filament change is provided during an interruption between the substrate and measuring grid layers.

The non-conductive substrate layer is based on PLA while a conductive compound filament (type: Protopasta Conductive PLA, Protoplant Inc., Vancouver, WA, USA) is used for the measuring grid layer. The compound (PLA-C) is primarily composed of PLA and electrically conductive carbon black. Its conductivity is dominated by the percolation mechanism. Here, the mobility of dispersed particles inside the material leads to a reconfiguration of the conductive path, and, thus, to a change in resistance [15].

Fabrication of the SG is done by using a 3D-printer (type: Prusa MK3s, Prusa Research a.s., Prague, Czech Republic) with a nozzle diameter of 0.4 mm and a printing bed temperature of 60 °C. The extruder temperatures for the substrate and measuring grid layers are 215 °C and 240 °C, respectively. The substrate layer consists of a single layer with a thickness of 0.2 mm, while the measurement grid consists of two layers with a thickness of 0.15 mm each. Two layers for the measurement grid were chosen to ensure a solid print without unwanted gaps that were present during visual inspections when printing only one layer. In order to evaluate the performance of the 3D-printed SG, it needs to be applied to a spring element. Here, a steel plate consisting of stainless steel (material no.: 1.4310) is used as spring element.

For determining a proper position for the 3D-printed SG that features a high strain in the range from 500 µm m^{-1} to 1000 µm m^{-1} while not exceeding the yield strength of the steel plate [16], a finite element analysis (COMSOL Multiphysics 5.6, COMSOL AB, SWE) is conducted. The finite element analysis (FEA) model consists of the steel plate with 3D-printed SG attached [Fig. 2(a)]. The Young's moduli of the steel plate, the PLA substrate and the PLA-C measuring grid are set to 186 GPa [17], [18], 3.12 GPa and 3 GPa [19], respectively. This steel plate is clamped at one end and loaded at a distance of 40 mm from this clamping with 30 N. The simulated strain along the steel plate shows a linear behavior [Fig. 2(b)] with an excessive strain at the clamping edge. Thus, the 3D-printed SG will be positioned at a distance of 10 mm from the clamping edge, i.e. avoiding the singularities area. This results in expected strains of the steel plate and printed SG of 415.4 µm m^{-1} and 490 µm m^{-1}, respectively.

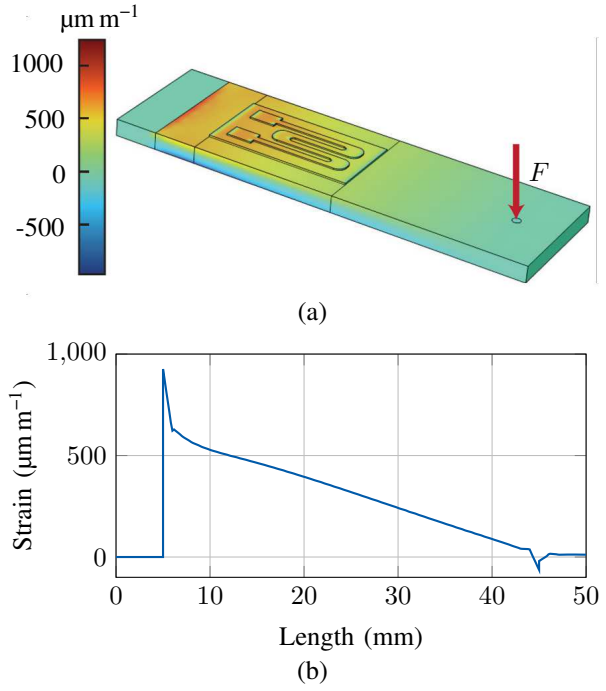

Fig. 2. Simulated strain along the steel plate for an applied load of 30 N, while the other end of the steel plate is clamped (a). The strain shows the expected behavior of a bending beam with the maximum strain at the clamping area (5 mm) and a linear decrease towards the loading end (b).

Finally, the 3D-printed SG is applied to the steel plate at the predetermined location. Therefore, the application area is prepared by sanding and subsequent cleaning with acetone. The mechanical connection of the 3D-printed SG is done by means of a cold curing superglue (type: Z70, HBK, Darmstadt, DE), which cures in about one minute under thumb pressure. This glue is especially used in experimental stress analysis applications. Electrical contact is established by melting copper wires into the contact pads using a soldering iron.

III. Analytic Modeling of the Static Behavior

The force F applied to steel plate results in a deflection at the contact point in negative z-direction and forms an angle φ with the horizontal plane. In case of small deflections, the displacement of the tip of the steel plate in x-direction can be neglected as well as the transverse contraction of the steel plate. The small deflection in z-direction is given by [20]

$$z = \frac{F L_{\text{eff}}^3}{3YI}, \text{ with } I = \frac{bh^3}{12}, \tag{1}$$

where L_{eff} is the effective length between the fixed point of the steel plate and the point of force application. Y and I are the Young's modulus and moment of inertia of the steel plate, respectively. The angle φ is given as [20]

$$\varphi = \frac{3}{2} \cdot \frac{z}{L_{\text{eff}}}. \tag{2}$$

Considering the difference of stiffness between the steel plate and the printed SG, it is valid to assume that the mechanical property of the assembly is defined solely by the steel plate. Thus, the neutral axis of the whole structure consisting of the steel plate, PLA substrate and PLA-C grid is in the center of the thickness of the plate. Since the center of the PLA-C grid is at a distance d from the neutral axis, the resulting strain of the grid in x-direction can be calculated as [21], [22]

$$\Delta L = d \cdot \varphi = \frac{d\, L_{\text{eff}}^2}{2YI} \cdot F. \tag{3}$$

The resistance change due to an applied force can be calculated as

$$\Delta R = S \cdot F, \text{ with } S = \alpha \cdot \frac{h L_{\text{eff}}^2}{2YI}, \tag{4}$$

where S is the sensitivity relating the force to the resistance change and α is the proportionality factor between the strain

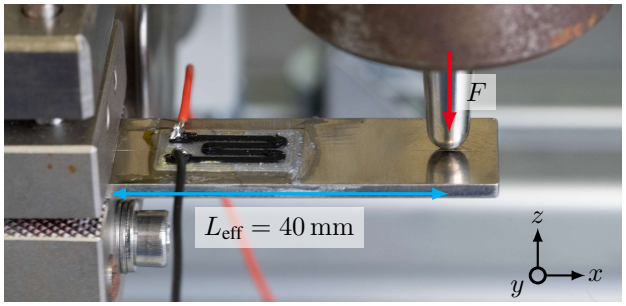

Fig. 3. Experimental setup for subjecting the steel plate with attached SG to a bending load.

of the PLA-C grid and change in resistance, which has to be determined experimentally.

IV. Experimental Setup for Static Loading

For evaluating the performance of the 3D-printed SG regarding its linearity and sensitivity, a bending load of 30 N is applied to the steel plate and the change in resistance ΔR of the 3D-printed SG is measured (Fig. 3). This involves clamping 5 mm from one end of the steel plate resulting in an effective beam length of 45 mm. The steel plate is loaded using a universal testing machine (type: inspekt table 5, Hegewald & Peschke, Nossen, DE) with a 100 N reference force sensor (type: S2M/100N with 0.02 % accuracy, HBK, Darmstadt, DE) via a spherical pin at a distance of 40 mm from the clamping. First, three full load cycles are performed to minimize settling. Then, the load is applied with a force-controlled slope of $0.2\,\text{N}\,\text{s}^{-1}$ followed by holding the load for 30 s and subsequent unloading with the same slope. This load profile is repeated four times. A digital multimeter (type: DMM 7510, Keithley, Cleveland, OH, US) is used to measure the resistance of the 3D-printed SG.

V. Results and Discussion

The bending load results in a correlating change in resistance ΔR of the 3D-printed SG upon which a creep is superimposed (Fig. 4). This creep results from the polymer properties of the filament as also reported in [23], which most likely is caused by a reorganization in conductive paths of the electrically conductive particles [23]. However, this needs further investigations of the material used, which are beyond the scope of this work. The loading and unloading of the steel plate lead to significant changes in resistances of $64.3\,\Omega \pm 1.3\,\Omega$ and $66.7\,\Omega \pm 1.8\,\Omega$ with a confidence interval of 95 %, respectively. These values are averaged over the four load cycles. Furthermore, the resistance-force characteristics for the loadings show a nearly linear behavior with correlation coefficients R^2 of 0.996 [Fig. 5(a)]. The linearity error of the loadings is within $\pm 4\,\%$ [Fig. 5(b)].

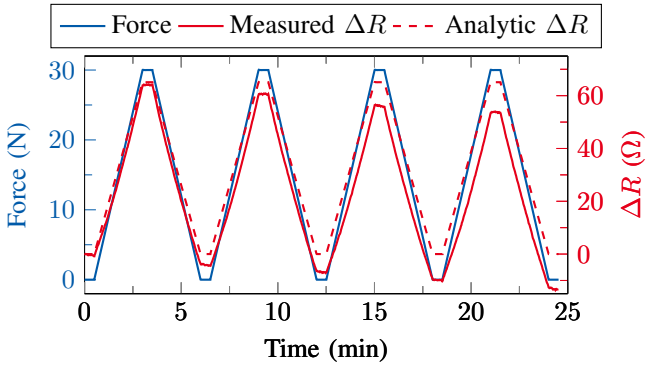

Fig. 4. The measured and analytic change in resistance correlate directly with the applied force of 30 N and result in changes of $64.3\,\Omega \pm 1.3\,\Omega$ and $66.7\,\Omega \pm 1.8\,\Omega$ for the loading and unloading cycle, respectively. A nearly linear drift of the measured resistance over time is present.

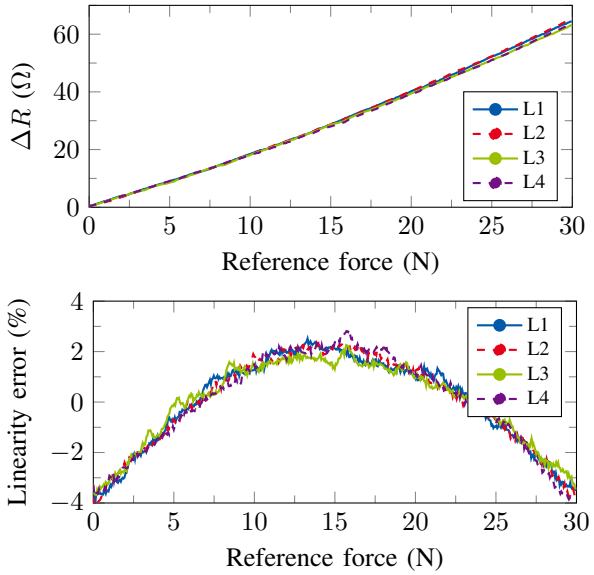

Fig. 5. The four loadings L1 - L4 show a nearly linear response of the change in resistance of the 3D-printed strain gauge with correlation coefficients R^2 of 0.996 (a). The linearity error of the loadings is within $\pm 4\,\%$ (b).

The gauge factor k of the 3D-printed SG is calculated by

$$k = \frac{\Delta R}{R_0} \cdot \frac{1}{\varepsilon_{\text{SG}}}, \tag{5}$$

where R_0 represents the base resistance of the 3D-printed SG. With a base resistance of 18 711.8 Ω, the changes in resistance (Fig. 4), and a strain of nearly $419.4\,\mu\text{m}\,\text{m}^{-1}$, which is in good agreement with the simulated strain of $416.7\,\mu\text{m}\,\text{m}^{-1}$, a gauge factor k of 8.3 results.

VI. Conclusion and Outlook

This work presents a method for manufacturing 3D-printed SGs based on a two-layer design by means of FFF that provide a cost-effective alternative to conventional SGs for stress analysis applications. Our experiments show that the 3D-printed SG is capable of measuring strain when bonded to a metal sprint element. A linear change in resistance is present under load with a sensitivity nearly four times higher compared to metal foil SGs. Future work is aimed at investigating and minimizing the creep of the 3D-printed SG to improve its accuracy and applicability.

REFERENCES

[1] A. K. Bose, X. Zhang, D. Maddipatla, S. Masihi, M. Panahi, B. B. Narakathu, B. J. Bazuin, J. D. Williams, M. F. Mitchell, and M. Z. Atashbar, "Screen-Printed Strain Gauge for Micro-Strain Detection Applications," *IEEE Sensors Journal*, vol. 20, no. 21, pp. 12652-12660, Nov. 2020.

[2] S. Zhang, L. Cai, W. Li, J. Miao, T. Wang, J. Yeom, N. Sepúlveda, and C. Wang, "Fully Printed Silver-Nanoparticle-Based Strain Gauges with Record High Sensitivity," *Advanced Electronic Materials*, vol. 3, no. 7, Jul. 2017.

[3] Q. Liang, K. Zou, J. Long, J. Jin, D. Zhang, G. Coppola, W. Sun, Y. Wang, and Y. Ge, "Multi-Component FBG-Based Force Sensing Systems by Comparison With Other Sensing Technologies: A Review," *IEEE Sensors Journal*, vol. 18, no. 18, pp. 7345-7357, Sep. 2018.

[4] M. L. Wymore, J. E. Van Dam, H. Ceylan, and D. Qiao, "A survey of health monitoring systems for wind turbines," *Journal of Lightwave Technology*, vol. 52, pp. 976-990, Dec. 2015.

[5] S. Keil, *Dehnungsmessstreifen*. Wiesbaden: Springer Fachmedien Wiesbaden, isbn: 978-3-658-13611-6, 2017.

[6] H.-R. Tränkler and L. Reindl, *Sensortechnik – Handbuch für Praxis und Wissenschaft*. Springer Vieweg Berlin Heidelberg, isbn: 978-3-642-29942-1, 2014.

[7] M. Borghetti, M. Serpelloni, and E. Sardini, "Printed Strain Gauge on 3D and Low-Melting Point Plastic Surface by Aerosol Jet Printing and Photonic Curing," *Sensors*, vol. 19, no. 19, Sep. 2019.

[8] M. Liu, Q. Zhang, Y. Shao, C. Liu, and Y. Zhao, "Research of a Novel 3D Printed Strain Gauge Type Force Sensor," *Micromachines*, vol. 10, no. 1, Dec. 2019.

[9] M. Liu, Y. Zhao, Y. Shao, Q. Zhang and C. Liu, "3D Printed Force Sensor with Inkjet Printed Piezoresistive Based Strain Gauge," in *Proc. IEEE Sensors*, Oct. 2018.

[10] H. L. Kao, C. L. Cho, L. C. Chang, C. B. Chen, W. H. Chung, and Y. C. Tsai, "A Fully Inkjet-Printed Strain Sensor Based on Carbon Nanotubes," *Coatings*, vol. 10, no. 8, Aug. 2020.

[11] H. Kang, S. Kim, J. Shin, and S. Ko, "Inkjet-Printed Flexible Strain-Gauge Sensor on Polymer Substrate: Topographical Analysis of Sensitivity," *Applied Sciences*, vol. 12, no. 6, Mar. 2022.

[12] N. Munasinghe, M. Woods, L. Miles and G. Paul, "3-D Printed Strain Sensor for Structural Health Monitoring," in *Proc. IEEE International Conference on Cybernetics and Intelligent Systems (CIS) and IEEE Conference on Robotics, Automation and Mechatronics (RAM)*, pp. 275-280, Nov. 2019.

[13] I. Mileti, L. Cortese, Z. Del Prete and E. Palermo, "Reproducibility and Embedding Effects on Static Performace of 3D Printed Strain Gauges," in *Proc. IEEE International Workshop on Metrology for Industry 4.0 & IoT*, pp. 499-504, Jun. 2021.

[14] M. Mathis, D. Vollberg, M. Langosch, D. Göttel, A. Lellig, and G. Schultes, "Novel method to reduce the transverse sensitivity of granular thin film strain gauges by modification of strain transfer," *Journal of Sensors and Sensor Systems*, vol. 9, no. 2, pp. 219-226, Jul. 2020.

[15] S. Kirkpatrick, "Percolation and Conduction," *Reviews of Modern Physics*, vol. 45, no. 4, pp. 574-588, Oct. 1973.

[16] J. Rausch, C. Hatzfeld, R. Karsten, R. Kraus, J. Millitzer, and R. Werthschützky, "Strain measurement on stiff structures: experimental evaluation of three integrated measurement principles," *Smart materials and structures*, vol. 21, no. 6, May 2012.

[17] R. Chadda, M. Link, T. Engel, C. Hartmann, O. Ben Dali, J. Probst, H. Merschroth, E. Abele, M. Weigold, and M. Kupnik, "Evaluation of Additively Manufactured Parts in Disruptive Manner as Deformation Elements for Structural Integrated Force Sensors," *IEEE Sensors Journal*, vol. 22, no. 20, pp. 19249-19258, Oct. 2022.

[18] R. Chadda, J. Probst, C. Hartmann, M. Link, M. Hessinger, E. Abele, M. Weigold, and M. Kupnik, "Disruptive Force Sensor Based on Laser-based Powder-Bed-Fusion," in *Proc. IEEE Sensors*, Oct. 2020.

[19] A. Akbari, M. Jawaid, A. Hassan, and H. Balakrishnan, "Epoxidized natural rubber toughened polylactic acid/talc composites: Mechanical, thermal, and morphological properties," *Cover ImageJournal of Composite Materials*, vol. 48, no. 7, pp. 769-781, Mar. 2014.

[20] T. Beléndez, C. Neipp, and A. Beléndez, "Large and small deflections of a cantilever beam," *European Journal of Physics*, vol. 23, no. 3, May 2002.

[21] O. Ben Dali, P. Pondrom, G. M. Sessler, S. Zhukov, H. von Seggern, X. Zhang, and M. Kupnik, "Cantilever-based ferroelectret energy harvesting," *Applied Physics Letter*, vol. 116, no. 24, Jun. 2020.

[22] O. Ben Dali, H. von Seggern, G. M. Sessler, P. Pondrom, S. Zhukov, X. Zhang, and M. Kupnik, "Ferroelectret energy harvesting with 3D-printed air-spaced cantilever design," *Nano Select*, vol. 3, no. 3, pp. 713-722, Aug. 2021.

[23] S. Dul, A. Pegoretti, and L. Fambri, "Fused Filament Fabrication of Piezoresistive Carbon Nanotubes Nanocomposites for Strain Monitoring," *Frontiers in Materials*, vol. 7, Feb. 2020.